Na channel can both be described (over a wide range of solutions and concentrations) by the same reduced model with the same unchanging two parameters (dielectric coefficient and diameter) in which side chains are spheres (Ca channel = EEEE or EEEA; Na channel = DEKA). In the EEEE channel, Ca^{2+} selectivity is driven by charge/space competition in which selectivity arises from a balance of electrostatics and the excluded volume of ions in the crowded selectivity filter. Electrostatics selects Ca^{2+} over monovalent cations. Excluded volume selects Ca^{2+} over larger divalent cations. All these combine to create depletion zones in the ionic density profiles that are crucial determinants of the current carried by each ionic species.

2666-Pos

Energetic Variational Analysis *EnVarA* of Ions in Calcium and Sodium Channels

Robert S. Eisenberg[1], Yunkyong Hyon[2], Chun Liu[3].
[1]Department of Molecular Biophysics, Rush University Medical Center, Chicago, IL, USA, [2]Institute of Mathematics and its Applications, University of Minnesota, MN, USA, [3]Department of Mathematics, Pennsylvania State University, State College, PA, USA.

Selective binding in both calcium and sodium channels can be described (in many solutions and concentrations: Biophysical Journal (2007) 93:p.1960) by the same reduced model and unchanging two parameters (dielectric coefficient and diameter) despite the very different primary structure of the two proteins (Ca channel EEEA/EEEE; Na channel DEKA) and properties, even though amino-acid side-chains (E, D, etc.) are represented only as charged spheres. Monte Carlo *MC* simulations, reported in ~30 publications, work well (we think) because they do not specify structure as an input, independent of conditions. Rather, *MC*calculates the structure as an output, as a self-organized, induced fit of side-chains to ions (and vice-versa). **Structure is different in different solutions** in self-organized systems. Self-organized systems can be powerfully analyzed using the calculus of variations, specifically, energetic variational analysis (*EnVarA*). We optimize *both* action and dissipation integrals (Least Action and Maximum Dissipation Principles), motivated by Rayleigh, then Onsager who optimized just one, or the other. The resulting systems of coupled partial differential equations automatically satisfy the First and Second Laws of Thermodynamics and electrostatic Poisson equations, with physical boundary conditions that can produce flow. *EnVarA* extends Navier-Stokes equations to complex fluids containing deformable droplets (Journal of Fluid Mechanics (2004) 515:p.293). ***EnVarA* provides a seamless extension of conservative Hamiltonian systems** (perhaps at thermodynamic equilibrium) **to dissipative systems.***EnVarA* **is a** field theory of ions in channels and solutions with entropy, friction, and flow. *EnVarA* computes current where *MC* computes only binding. *EnVarA* applied to EEEE/DEKA channels gives binding like real calcium/sodium channels. Time dependent currents computed with *EnVarA* resemble time dependent currents in either voltage activated sodium or potassium (squid axon) channels (depending on parameters), **although the *EnVarA* model has only one unchanging conformation.**

2667-Pos

3D Structure of a Recombinant DHPR Expressed in Mouse

John Szpyt[1], Claudio F. Perez[1], Nancy Lorenzon[2], Ethan Norris[2], PD Allen[1], Kurt Beam[3], Montserrat Samso[1].
[1]Brigham & Women's Hospital/Harvard Medical School, Boston, MA, USA, [2]University of Colorado-Denver, Aurora, CO, USA, [3]University of Denver-Colorado, Aurora, CO, USA.

The dihydropyridine receptor (DHPR) is an L-type Ca^{2+} channel that acts as the voltage sensor for excitation-contraction coupling in skeletal muscle by tightly controlling the intracellular Ca^{2+} channel RyR1. Because previous 3D electron microscopic studies have largely not resolved the spatial organization of the DHPR subunits (α1s, α2-δ, β1a, and γ), we constructed mice expressing a β1a subunit with YFP and a biotin acceptor domain attached to its N- and C- termini respectively. This engineered β1a sustains a functional DHPR-RyR1 interaction and viable animals in a β1a null background. DHPRs were purified from mice by means of the (biotinylated) biotin acceptor domain, negatively stained and imaged with electron microscopy. 8,662 individual DHPRs were analyzed using single-particle image processing algorithms. Multivariate statistical analysis, classification, and multi-reference alignment yielded distinct 2D class averages corresponding to different orientations of the macromolecule. The 3D reconstruction, with 25 Å resolution, shows two distinct parts: a main body shaped like an irregular pentagon (~150x125x75 Å) with distinct corners, and a hook-shaped feature that extends ~60 Å from the main body. Consistent with the considerable conservation of membrane topology among voltage-gated channels, a good part of the main body can be closely fitted with an atomic structure of a full-length potassium channel, suggesting that the main body contains the α1s subunit. Besides the fitted potassium channel the main body has extra volume that can accommodate the YFP atomic coordinates and other subunits.

Supported by NIH/NIAMS (AR055104) to KGB and NIGMS (GM081819) to PDA.

2668-Pos

$Ca_v2.3$ Calcium Channels Inactivate from the Open State with Partial Charge Immobilization and Altered Deactivation Kinetic

Gustavo Contreras[1], Alan Neely[2].
[1]Doct. en Neurociencia. U. de Valparaiso, Valparaiso, Chile, [2]C. Inderdisc. de Neurociencia de Valpo. U. de Valparaiso, Valparaiso, Chile.

Voltage-dependent ion channels undergo inactivation following activation. In the sodium and potassium channels, the molecular determinants that govern the mechanism of inactivation involve pore blocking by a cytoplasmic particle. In calcium channels the consensus model is that the intracellular loop joining the first two homology domains of the pore forming subunit contributes to the inactivation gate or hinged-lid. To investigate key features of this model, we expressed $Ca_V2.3$ channel in *Xenopus oocytes* without auxiliary subunits and recorded ionic and gating currents using the cut-open voltage-clamp technique. Ionic current were recorded in either Ba^{2+} or Ca^{2+}. Here we report that consistent with a hinge-lead mechanisms, charge movement at the end of a depolarizing pulse decreases up to a 50% with channel inactivation. In contrast with a previous report by Patil et al (1998, Neuron 20:1020) that co-expresses auxiliary subunit with $Ca_V2.3$, trains of pulse elicited minimal inactivation. It appears then that when expressed alone, $Ca_V2.3$ channels inactivate mostly from the open state. We also found that as channels inactivate, a slow component emerges in tail-current recordings. This component contributes to about 20% of the tail currents in 80% inactivated currents and can be accounted for with a classic allosterically-coupled model provided that channels can re-open multiple times from the last closed state and that some closed-inactive channels reopen during membrane repolarization.

Supported by REFD-24 and FONDECYT 1980635 to AN and a CONICYT Fellowship to GC.

2669-Pos

Action Potential Hyperpolarization Kinetics Abets the Modulation of Alpha1h T-Type Calcium Channels by KLHL1 Mutants Lacking the Actin-Binding Domain (ΔKelch)

Kelly A. Aromolaran, Erika S. Piedras-Renteria.
Loyola University Chicago, Maywood, IL, USA.

The Kelch-like 1 protein (KLHL1) is a neuronal actin-binding protein that increases the current density and channel number of $Ca_v3.2$ calcium channels *via* actin-F mediated increases in recycling endosomal activity. Removal of the actin-binding kelch motif (ΔKelch) prevents the increase in α_{1H} current density seen with wild-type KLHL1 when tested with square pulse protocols but not the increase in calcium influx seen during action potentials (AP).

Here we set out to dissect the kinetic properties of AP that confer the mutant kelch the ability to interact with α_{1H} and induce an increase in calcium influx. Square waveforms (black trace) following the AP did not significantly increase calcium influx (25%, $p>0.05$) compared to the AP (red). We investigated the effects of altering the slope of the repolarization (1), the length of hyperpolarization (2), the slope of repolarization from hyperpolarization (3) and the duration of depolarization (4) on the modulation of α_{1H} by ΔKelch. Our results show that the slope of repolarization from hyperpolarization induces the conformational changes that allow the channel to properly interact with ΔKelch, leading to increased Ca influx.

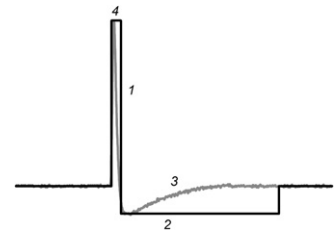

2670-Pos

C-terminal Alternative Splicing Modulates Single-Channel Gating of $Ca_v1.3$ L-Type Calcium Channel

Wanchana Jangsangthong[1], Jan Petran[1], Anamika Singh[2], Jörg Strissnig[2], Stefan Herzig[1], Alexandra Koschak[2].
[1]University of Cologne, Cologne, Germany, [2]University of Innsbruck, Innsbruck, Austria.

We have recently discovered a novel mechanism of channel modulation in $Ca_V1.3$ channels enabling cells to tightly control gating by C-terminal alternative splicing. The absence of a C-terminal modulatory motif (CTM) within a short splice form facilitates $Ca_V1.3$ channel activation at lower voltages and induces pronounced Ca^{2+} dependent-inactivation (CDI) (Singh *et al*., JBC 2008). Intriguingly, whole-cell measurements revealed a significant

difference in current density between long and short channels for both Ba^{2+} and Ca^{2+} currents (I_{Ba} and I_{Ca}) while membrane expression of the pore-forming subunit was unchanged suggesting additional differences of unitary current properties. To further determine the mechanism underlying CTM modulation, we performed single-channel analysis of recombinant long ($Ca_V1.3_{42}$) or short ($Ca_V1.3_{42A}$) channels co-expressed with β_3 and $\alpha_2\delta$-1 in HEK-293 cells using either15mM Ba^{2+} or Ca^{2+} as charge carrier. We found a significant increase of channel availability given as fraction of active sweeps [%] (at −30mV for $Ca_V1.3_{42}$: 20.9 ± 3.1, $Ca_V1.3_{42A}$: 60.9 ± 9.7, $p<0.01$, Students t-test) which reflects the shift to hyperpolarized potentials of $Ca_V1.3_{42A}$ channels in whole-cell experiments. Furthermore, larger currents in $Ca_V1.3_{42A}$ channels were due to significantly increased open probability across all test potentials. Single-channel conductance was similar (16 and 15 pS for $Ca_V1.3_{42}$ and $Ca_V1.3_{42A}$). The inactivation of ensemble average I_{Ba} was similarly slow in both channels. In contrast, more pronounced single-channel I_{Ca} inactivation of $Ca_V1.3_{42A}$ compared to $Ca_V1.3_{42}$ was found (τ_{inact} [ms] at −10mV: $Ca_V1.3_{42}$: 35.5 ± 12.3, $Ca_V1.3_{42A}$: 8.2 ± 3.1).Taken together, single-channel properties reflect the differences in voltage- and Ca^{2+}-dependent activation and inactivation gating properties previously observed in whole-cell recordings for these two splice variants. We could explain the higher current density of $Ca_V1.3_{42A}$ channels by increased channel activity.

Support: FWF P-20670 to J.S.; University of Innsbruck to A.K.; and CMMC A4 University of Cologne to S.H.

2671-Pos

Both Voltage- and Ca^{2+}-Dependent Inactivation of $Ca_v1.2$ Ca^{2+} Channels are Suppresed in Myotubes, Likely Because of Triad Junction Proteins other than RyR1

Joshua D. Ohrtman[1], Kurt G. Beam[1], Paul D. Allen[2].
[1]University of Colorado Denver, Aurora, CO, USA, [2]Brigham and Women's Hospital, Boston, MA, USA.

To investigate the relationship between calcium channel and EC coupling functions of CaV1.1 in skeletal muscle, we have compared its behavior with that of the cardiac L-type channel, CaV1.2. Using expression in tsA-201 cells, we showed that substituting CaV1.1 IQ motif residues into CaV1.2 IQ caused a loss of calmodulin binding and calcium-dependent inactivation (JBC 283:29301-11, 2008), raising the possibility that inactivation is maladaptive for CaV1.1 function in muscle. We thus compared inactivation of CaV1.2 in tsA-201 cells and *dysgenic* myotubes (null for CaV1.1). For CaV1.2 in tsA-201 cells (co-expressed with $\alpha2\delta1$ and $\beta2a$), $I_{50\ ms}/I_{peak}$ (R_{50}) at +20 mV was .69 in 10 Ca and .87 in 10 Ba, whereas R_{50} for CaV1.2 in dysgenic myotubes was .95 at +20 mV in 10 Ca, indicating that both voltage- and calcium-dependent inactivation were suppressed. In tsA-201 cells, co-expression of $\beta1a$ (the predominant skeletal muscle isoform) did not significantly alter R_{50} values from those with $\beta2a$. Furthermore, R_{50} values were similar for CaV1.2 expressed in *dysgenic* myotubes and myotubes null for both CaV1.1 and RyR1, suggesting that some component of muscle triad junctions other than RyR1 is responsible for the suppression of inactivation. We thus expressed CaV2.1 in *dysgenic* myotubes because this neuronal channel, unlike CaV1.2, is not targeted to triad junctions (PNAS 95:1903-1908, 1998). Consistent with the hypothesis CaV2.1 channels showed significant voltage- and calcium-dependent inactivation in *dysgenic* myotubes which were similar to those of the channel expressed in tsA-201 cells. We are currently seeking to identify the components involved in suppressing inactivation of CaV1.2 in myotubes. Supported by AHA0190016G to JDO and NIH/NIAMS (AR055104) and MDA4319 to KGB.

2672-Pos

Electromechanical Coupling During the Activation of $Ca_v1.2$

Sebastien Wall-Lacelle, Yolaine Dodier, Alexandra Raybaud, Rémy Sauvé, Lucie Parent.
University of Montreal, Montreal, QC, Canada.

The $Ca_V\alpha_1$ subunit of L-type calcium channel $Ca_V1.2$ is formed of a voltage sensing domain (segments S1 to S4) and a pore-forming domain (segments S5-S6). Although the electromechanical coupling between these regions during opening and closing of the channel, in which movement of the S4 voltage sensor is mechanically transferred to the gate via movement of the S4-S5 linker, has been well established in K^+ channels (Long et al. 2005), the molecular mechanism linking the movement of the voltage sensor to the opening of the pore remains elusive in voltage dependent Ca^{2+} channels. Glycine mutations at position I781 in the distal IIS6 helix in $Ca_V1.2$ (Timin et al., 2009) and the equivalent I701 residue in $Ca_V2.3$ (Raybaud et al., 2007) have been shown to significantly decrease the free energy of voltage-dependent activation in both channels, suggesting that IIS6 plays a key role in coupling the pore opening and the voltage-sensing domain. To examine the electromechanical model of channel opening in $Ca_V1.2$, cross-linking studies were undertaken with pairs of cysteine mutants introduced in the S4-S5 linker(s) and I781C in IIS6. The biophysical properties of the double mutants expressed in *Xenopus* oocytes, are currently tested in the presence of the bridging reagent $tbHO_2$ at 0.5 mM. We hypothesize that if cysteine residues in the S4-S5 linker come in atomic proximity ($\leq$ 3 Å) with I781 during channel activation, addition of $tbHO_2$ will promote the formation of a disulfide bridge. This effect should be reversible by addition of DTT. Supported by grants from the Canadian Institutes of Health Research and the Heart and Stroke Foundation of Canada to LP.

2673-Pos

Activation Gating Determinants in Segments IS6 - IIIS6 of $Ca_v1.2$

Stanislav Beyl, Annette Hohaus, Eugen Timin, Steffen Hering.
Pharmacology and Toxicology, Vienna, Austria.

We have previously shown that mutations in pore lining segment IIS6 of Cav1.2 induce leftward shifts of the activation curve reflecting a destabilization of the closed and a simultaneous stabilization of the open channel state (Beyl et al. 2009). Systematic substitutions of a cluster of hydrophobic residues (LAIA motive) by residues of different size and polarity (except proline) revealed a strong correlation between changes in hydrophobicity (ΔH) and the shifts of the activation curve ($\Delta V_{0.5}$). A similar analysis in segment IS6 revealed no correlation between ΔH and $\Delta V_{0.5}$. Here we show that amino acid substitutions in the corresponding sequence stretch of segment IIIS6 (F1191 - I1196) shift the activation curves ($\Delta V_{0.5}$ F1191T=-7.1 ± 1.3mV, V1192T= 8.2 ± 1.2mV , G1193T=-31.2 ± 1.3mV, F1194T=2.1 ± 1.2mV, V1195T= -10.3 ± 1.1mV, I1196T=-17.9 ± 1.1mV). A reduction in hydrophobicity in positions V1195 (ΔH(V1195T)=-4.9) and I1196 (ΔH(I1196T)=-5.2) apparently destabilized the closed channel state. Other mutations (V1192T, G1193T and F1194T) did not fit this paradigm. Potential interactions between residues in segments IS6, IIS6 and IIIS6 were analysed by means of double mutant cycle analysis. Our data reveal a positional specific interaction between gating determinants in segments IS6 and IIS6 as well as IIS6 and IIIS6. Rate constants of the voltage sensing machinery and pore stability were estimated using a 4 state gating model (Beyl et al. 2009).

2674-Pos

Effects of Alanine Substitutions for Highly-Conserved Phenylalanines in the Skeletal Muscle L-Type Calcium Channel

Roger A. Bannister[1], Ong Moua[1], Joshua D. Ohrtman[1], Chris A. Ahern[2], Kurt G. Beam[1].
[1]University of Colorado-Denver, Aurora, CO, USA, [2]University of British Columbia, Vancouver, BC, Canada.

The motif FxxExxxK/R is highly conserved in S2 segments of voltage-gated cation channels, including the four repeats of the α_{1s} subunit of the skeletal muscle L-type Ca^{2+} channel, and appears to represent an important structure for voltage-sensing. Moreover, mutating the conserved S2 phenylalanine within the drk1 K^+ channel monomer to alanine causes a ~50 mV depolarizing shift in activation (Li-Smerin et al., JGP 115:33-49). Here, we made homologous F to A substitutions in Repeat I (F97A), Repeat III (F843A) and Repeat IV (F1161A) of α_{1S} N-terminally tagged with yellow fluorescent protein (YFP-α_{1S}), and tested the ability of the mutants to conduct L-type Ca^{2+} current and serve as the voltage sensor for excitation-contraction (EC) coupling after expression in *dysgenic* (α_{1S} null) myotubes. Confocal imaging of the YFP tag indicated that each of these constructs was targeted to plasma membrane junctions with the sarcoplasmic reticulum (SR). Measurement of intramembrane charge movements showed no significant difference in mutant expression relative to YFP-α_{1S} ($p > 0.05$, *ANOVA*). The F843A and F1161A mutants both supported L-type currents and myoplasmic Ca^{2+} transients with similar amplitude and voltage-dependence to those of YFP-α_{1S}. In contrast, the F97A mutant displayed substantial depolarizing shifts in activation of L-type current (24 mV) and SR Ca^{2+} release (13 mV). Together, these results indicate that: *i*) voltage-induced conformational changes in repeat I are directly important for activation of both L-type current and EC coupling, and *ii*) either repeats III and IV are less directly important for these functions or the F-A mutations have little influence on voltage-dependent conformational changes of these repeats. We are currently assessing the effects of the F475A mutation in Repeat II. Supported by NIH AR055104 and MDA4319 to K.G.B. and MDA4155 to R.A.B.